Available online at www.sciencedirect.com
ScienceDirect
Journal of Hazardous Materials 156 (2008) 141–147
Journal of Hazardous Materials
www.elsevier.com/locate/jhazmat

Optimized coverage of gold nanoparticles at tyrosinase electrode for measurement of a pesticide in various water samples

Gha-Young Kim [a], Joonmok Shim [b], Min-Su Kang [b], Seung-Hyeon Moon [b,*]

[a] *International Environmental Research Center, South Korea*
[b] *Department of Environmental Science and Engineering, Gwangju Institute of Science & Technology (GIST), 261 Cheomdan-Gwagiro, Buk-gu, Gwangju, 500-712, South Korea*

Received 16 September 2007; received in revised form 4 December 2007; accepted 4 December 2007
Available online 8 December 2007

Abstract

Gold nanoparticles (AuNPs) were electrodeposited onto a glassy carbon (GC) electrode to increase the sensitivity of the tyrosinase (TYR) electrode. By controlling the applied potential and time, the coverage of AuNPs at the TYR electrode was optimized with respect to the current response. The voltammetric measurements revealed a sensitive enzymatic oxidation and electrochemical reduction of substrate (phenol and catechol). The quantitative relationships between the inhibition percentage and the pesticide concentration in various water samples were measured at the TYR-AuNP-GC electrode, showing an enhanced performance attributed by the use of AuNPs.

Keywords: Gold nanoparticle; Electrodeposition; Double-pulse technique; Tyrosinase electrode; Pesticide

1. Introduction

Pesticides are among the important environmental pollutants. Since these are toxic and carcinogenic even at low concentration [1–8], a development of analytical methods for a quick analysis or an on-line monitoring is required to measure pesticides. Instead of the traditional off-line measurements, enzyme electrode is reliable technique for fast screening of pesticides. Despite the advantages such as simplicity, selectivity, and easy miniaturization, the enzyme electrode has limited sensitivity for application in detecting low-concentration pesticides [9,10].

Recently comprehensive studies on the improvement of the performance of an enzyme electrode by introducing gold nanoparticles were reported [11–13]. Because gold is environmentally benign noble metal in comparison with other metals and the nanoparticle (AuNP) is playing a significant role in the biosensors allowing the communication between enzyme and electrode materials [14–19]. For these reasons, it is expected that the use of AuNP can lead to enhancement of the performance of enzyme electrode for detection of pesticides at low concentration. Among the various methods for introducing gold nanoparticles, the electrochemical deposition method is more attractive in electrode modification by enhancing the electrode conductivity, facilitating the electron transfer and improving the analytical sensitivity and selectivity [20–22]. The method does not need a separate procedure because the formation and deposition of nanoparticles on the electrode surface occurred at the same time. In addition, double-pulse deposition is an effective way to control the particle size distributions of depositions [23].

In this study, the AuNPs were electrodeposited by double-pulse to improve the performance of tyrosinase (TYR) electrode for measurement of pesticides. The effects of the applied potential and time on the particle size and coverage were investigated. The AuNPs were modified with the formation of self-assembled monolayer (SAM), followed by the immobilization of TYR. The optimum coverage on the current response of the prepared electrode was examined. The electrode was characterized by the cyclic voltammetry (CV) measurements and tested for atrazine by amperometric measurements.

2. Experimental

2.1. Materials

Potassium tetarachloroaurate (III) ($KAuCl_4$), potassium ferricyanide ($K_3Fe(CN)_6$), potassium chloride (KCl), sulfuric acid

* Corresponding author. Tel.: +82 62 970 2435; fax: +82 62 970 2434.
E-mail address: shmoon@gist.ac.kr (S.-H. Moon).

0304-3894/$ – see front matter © 2007 Elsevier B.V. All rights reserved.
doi:10.1016/j.jhazmat.2007.12.007

(H_2SO_4, 0.5 M), tyrosinase (from mushrooms, EC 1.14.18.1, 50,000 units/mg), 3-mercaptopropionic acid (MPA), ethanol, *N*-(3-dimethylaminopropyl)-*N*′-ethylcarbodiimide hydrochloride (EDC), *N*-hydroxysuccinimide (NHS), catechol, phenol, and atrazine (2-chloro-4-ethylamino-6-isopropylamino-1,3,5-triazine), were supplied by Sigma–Aldrich (USA). All the chemicals used in this study were analytical reagent grade.

2.2. Apparatus

The deposition and voltammetric experiments were performed in a Teflon cell of 5 mL volume using a three-electrode. The cell was connected with a PGSTAT30/GPES system (Autolab, Netherlands). A glassy carbon (GC) electrode was used as working electrode. A BAS MF 2030 Ag/AgCl reference electrode and a Pt wire counter electrode were also employed. All potentials in the text are expressed against NHE. Amperometric response to pesticides was measured in a thin-layer flow cell (volume = 21 μL, BAS, West Lafayette, IN, USA) at 0.23 V vs. NHE, which was determined from CV measurements and 5 μL of the test solution was delivered through a loop (Rheodyne, USA). The geometrical area of GC electrode was measured in $Fe(CN)_6^{3-/4-}$ according to the Cottrell equation. The coverage of TYR-AuNP-GC electrode used in the characterization was about 13%.

2.3. Preparation of AuNPs-GC electrode

The deposition of AuNPs was performed onto the surface of pretreated GC electrode in the deaerated $KAuCl_4$ solution by applying potential for a programmed time period using a double-pulse technique. The deposited surface area of AuNP was calculated from charge corresponding to the reduction of gold oxides formed by CV [24].

2.4. Preparation of TYR-AuNP-GC electrode

The AuNP-GC electrode was pretreated with a fresh piranha solution (H_2O_2:H_2SO_4 = 3:7, v/v) at 80 °C for 5 min and immersed in deaerated 20 mM of MPA in ethanol/distilled water (75:25, v/v) to form a SAM layer for 24 h at room temperature under darkness. After rinsing of the modified electrode with ethanol and distilled water, enzyme was immobilized on the SAM layer by covalent bond with the use of EDC (0.2 M) and NHS (0.05 M). EDC converted the carboxyl group to an unstable amine-reactive intermediate, and NHS was used to prevent the hydrolysis of the unstable intermediate. Prior to the electrochemical measurements, the electrode was thoroughly washed with phosphate buffer solution (PBS, 0.1 M, pH 7).

2.5. SEM analysis

Scanning electron microscopy analysis of the AuNP deposits was carried out using a FESEM (S-4700, Hitachi, Japan) at an acceleration voltage of 15–20 kV and a working distance of 4–5 mM.

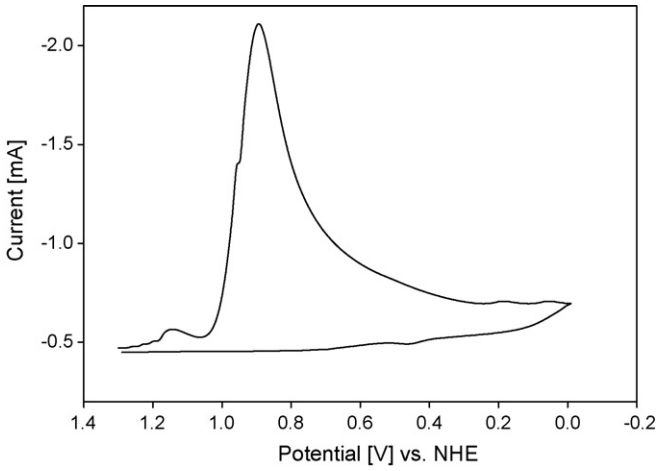

Fig. 1. Cyclic voltammograms of GC electrode for $KAuCl_4$ (0.2 mM) in H_2SO_4 (0.5 M) at 100 mV/s.

3. Results and discussion

3.1. The effect of nucleation potential (E_1) and time (t_1)

In double-pulse deposition, the first pulse (E_1) was used to initiate the formation of nuclei, and the second pulse (E_2), was used to control the growth of the nuclei formed during the previous pulse. Nucleation is a critical process in metal deposition for the formation of a new crystal and the growth of a perfect singular crystal face by formation of new layers [25]. The driving force of nucleation can be varied by simply varying the applied potential. As a preliminary experiment for determining the nucleation potential, cyclic voltammetric measurement was performed using a GC electrode for the Au colloid solution.

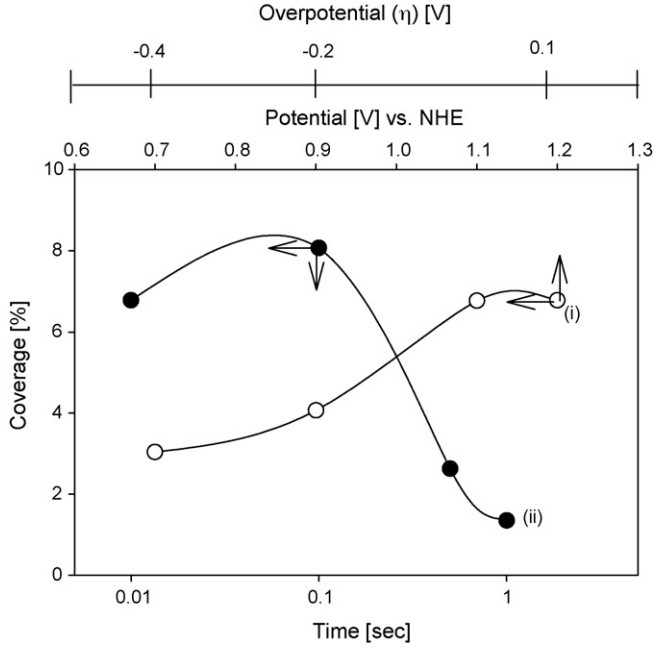

Fig. 2. The effect of the nucleation potential (E_1) (curve (i)) and time (t_1) (curve (ii)) on the coverage of AuNPs ([$KAuCl_4$] = 0.2 mM, E_2 = −0.2 V vs. NHE, t_2 = 60 s).

As shown in Fig. 1, an initial cathodic current at 1.1 V and a sharp peak at 0.9 V corresponding to the reduction of adsorbed $AuCl_4^-$ and solution bound Au (III) to Au (0), respectively. This voltammetric adsorption of Au complexes to carbon electrodes has been observed previously [26–28]. No anodic peak is observed on the reverse scan indicating the irreversibility of the reduction of $AuCl_4^-$.

The effect of nucleation potential and time was observed under a growth condition, $E_2 = -0.2$ V vs. NHE and $t_2 = 60$ s, at a constant nucleation time ($t_1 = 0.1$ s) and a constant nucleation potential ($E_1 = 1.2$ V vs. NHE), respectively. In Fig. 2, curve (i) shows the effect of an applied nucleation potential (E_1) on the coverage of AuNPs. As the nucleation potential increased, the coverage increased but no significant influence on the particle size was observed for nucleation time of 0.1 s (data not shown). This may be expected because t_1 (0.1 s) is negligible in comparison to t_2 (60 s), such that differences in the particle size immediately after t_1 were leveled off by the applied growth potential [23]. As shown in curve (ii) in Fig. 2, a high coverage was obtained at $t_1 = 0.1$ s, and beyond that it decreased. Dimensionless current transients were plotted and SEM measurements were conducted for different t_1. As shown in Fig. 3, an instantaneous and progressive nucleation was found at $t_1 = 0.01$ s and 0.1 s, respectively. At a time longer than 0.1 s, the nucleation follows neither instantaneous nor progressive development. The instantaneous nucleation maximizes particle size monodispersity, but it is desirable to grow particles (progressive nucleation) to control diffusion zone coupling to prevent the screening of the expanding diffusion fields around existing nuclei [29]. Therefore optimal potential and time of the nucleation was selected as 1.2 V vs. NHE and 0.1 s.

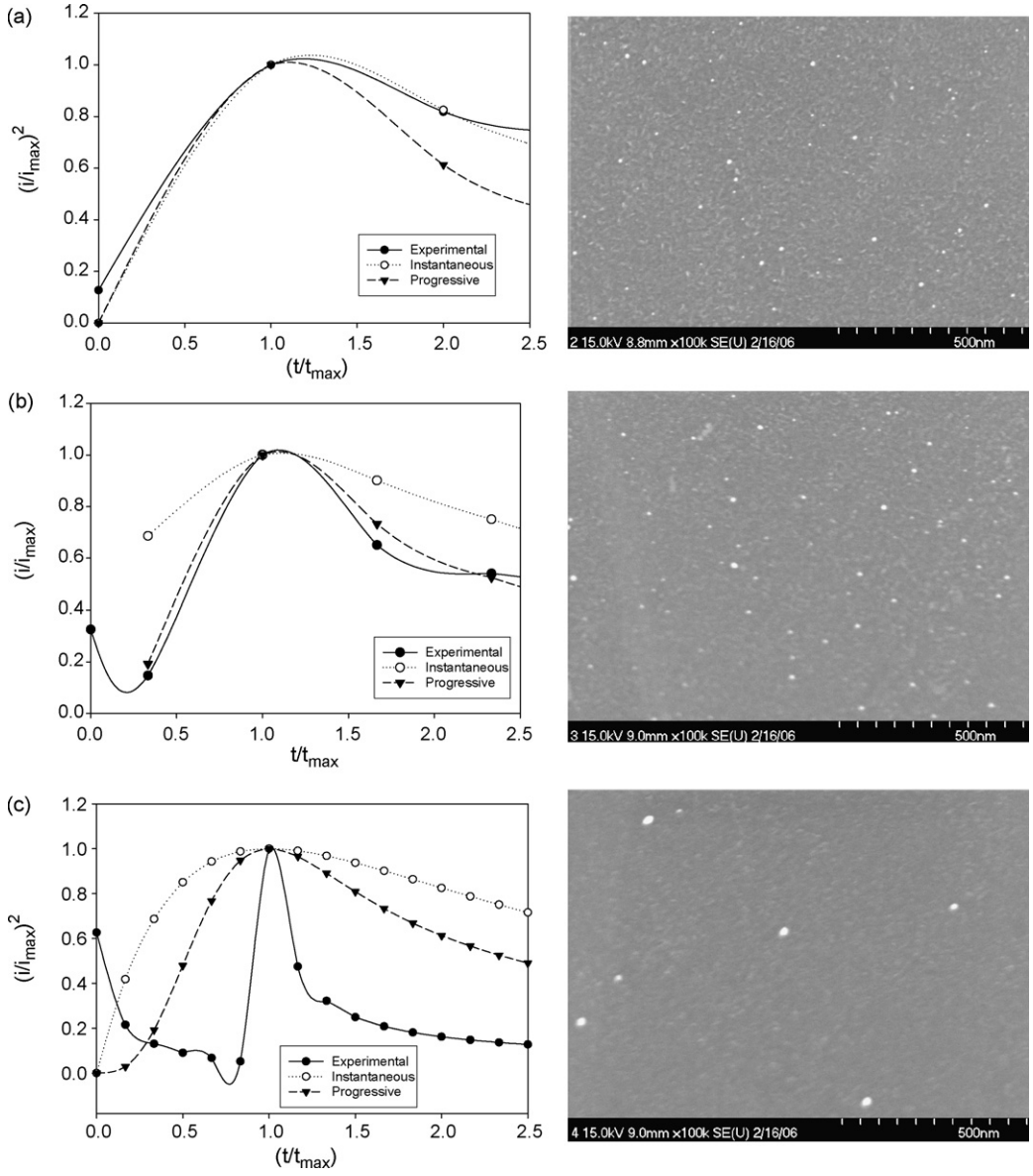

Fig. 3. Current transient plots and SEM photographs at different nucleation time, (a) 0.01 s, (b) 0.1 s, and (c) 1 s ([$KAuCl_4$] = 0.2 mM, $E_1 = 1.2$ V vs. NHE, $E_2 = -0.2$ V vs. NHE, $t_2 = 60$ s).

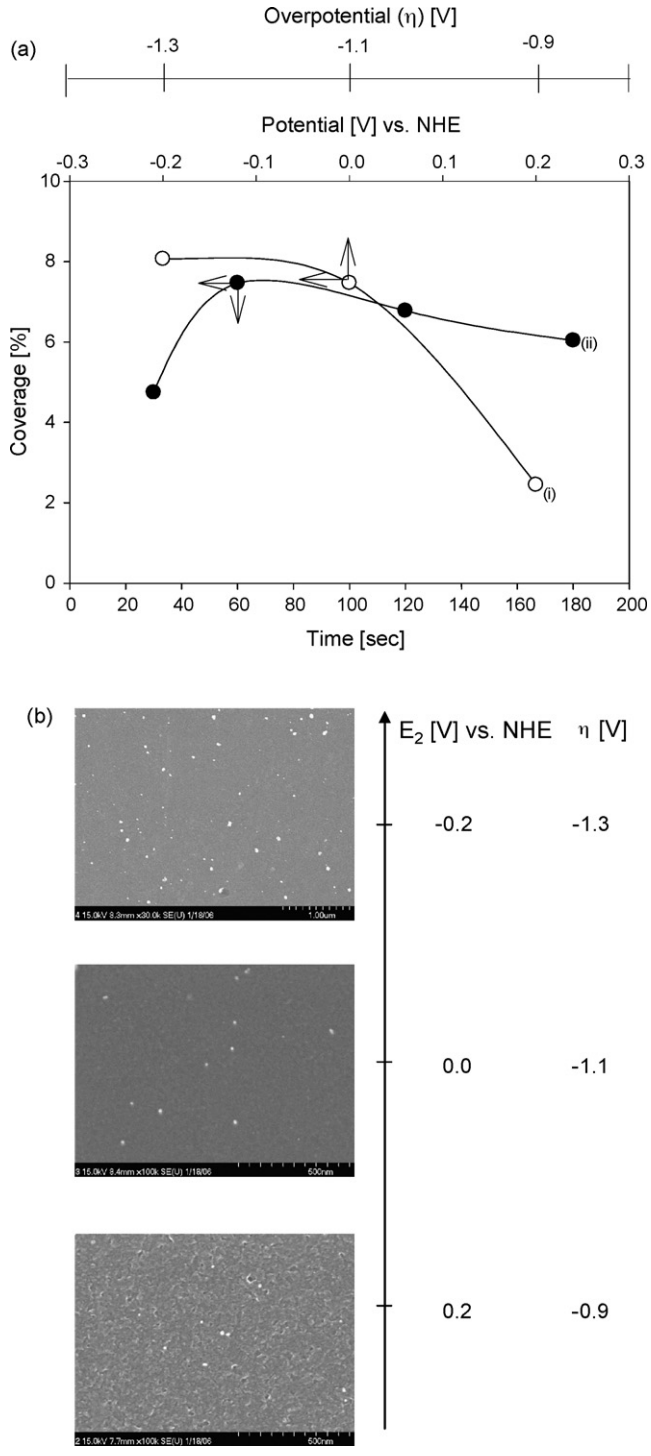

Fig. 4. The effect of the E_2 (curve (i)) and t_2 (curve (ii)) on the coverage of AuNPs (a) and SEM photographs (b) ([$KAuCl_4$] = 0.2 mM, E_1 = 1.2 V vs. NHE, t_1 = 0.1 s).

3.2. The effect of growth potential (E_2) and time (t_2)

The effect of the growth potential on the coverage of AuNPs was investigated. As shown in Fig. 4 (a), the coverage increased with a negative increase in the growth potential (E_2) (increasing overpotential). From the SEM photographs (Fig. 4 (b)), increase in the number of visible AuNPs with negatively increasing E_2 was observed. Since growth potential is related with the particle size in a double-pulse deposition, a sufficient growth potential should be supplied to grow efficient size of particles although nuclei were formed within a nucleation step. In addition, the coverage increased with increasing growth time (t_2) to 60 s, but a tendency for a decreasing coverage was observed with further increasing due to a destabilization of the cluster [22].

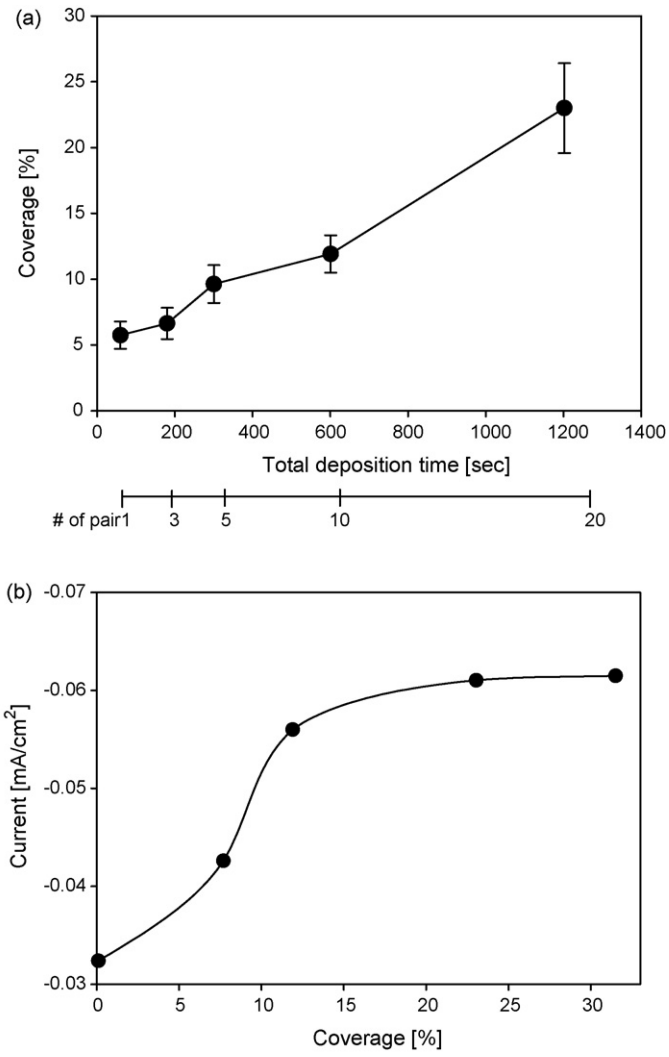

Fig. 5. (a) The effect of total deposition time on the coverage of AuNPs and (b) the effect of coverage on the current response of TYR-AuNP-GC electrode for1 mM catechol in O_2-saturated PBS (0.1 M, pH 7) at 0.23 V vs. NHE.

3.3. The effects of total deposition time and coverage

Based on the obtained conditions, AuNPs deposited GC electrode was prepared by applying multiple pairs of double-pulse. Fig. 5(a) shows the increase of coverage with the total deposition time (or number of pulse pairs). As the coverage increased until around 13%, the current response of TYR-AuNP-GC electrode increased, while further increase of the coverage does not induce enhancement of current signal (Fig. 5(b)). It was assumed that the further increase of the coverage did not enhance the interaction of the enzyme with the electrode due to

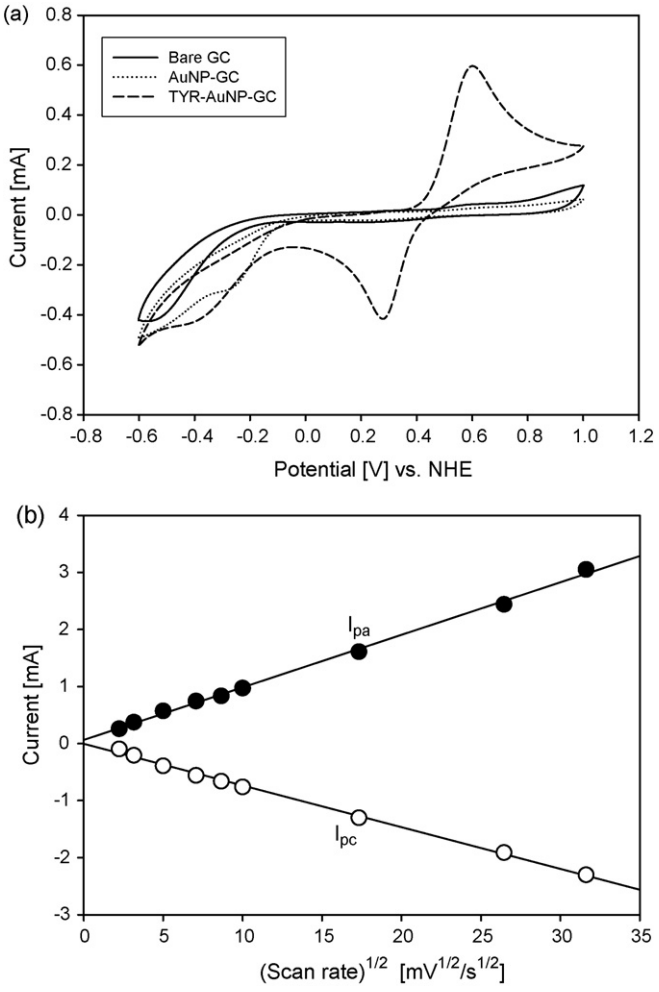

Fig. 6. (a) Cyclic voltammograms of bare, AuNP-, and TYR-AuNP-GC electrode for 1 mM of phenol in O_2-saturated PBS (0.1 M, pH 7) at 25 mV/s and (b) the linear relationship of I_{pa} and I_{pc} with (scan rate)$^{1/2}$.

the possible existence of the attractive Van der Waals interaction and repulsive electrostatic interaction between neighboring bio-macro-molecules [30].

3.4. Characterization of TYR-AuNP-GC electrode

A detection of phenol, which is typically used as a substrate, at the prepared TYR electrode was examined by the measurements of cyclic voltammograms. As shown in Fig. 6(a), there were no significant redox peaks at the bare and AuNP-GC electrodes. However, in the case of TYR-AuNP-GC electrode, an anodic and a cathodic peak were observed near 0.6 and 0.2 V vs. NHE, respectively. These coincide with the redox peak potential of catechol. That is, the phenol was oxidized by tyrosinase and converted to catechol. It was further oxidized by enzymatic reaction as well as electrochemical reaction with generation of quinone. Therefore the anodic peak was due to the electrochemical oxidation of catechol, which is the oxidation product of phenol by tyrosinase (Scheme 1). However, the cathodic peak was due to the reduction of quinone, which was the oxidation product of catechol (or phenol) not only by the electrochemical

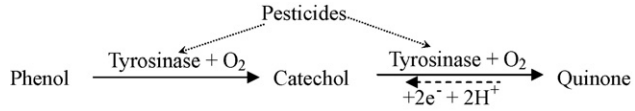

Scheme 1. The enzymatic oxidation and electrochemical reduction at tyrosinase electrode.

Table 1
The electrochemical properties of bare, AuNP-, and TYR-AuNP-GC electrodes for 1 mM of catechol in O_2-saturated PBS (0.1 M, pH 7) at 25 mV/s

Type of electrode	Bare GC	AuNP-GC	TYR-AuNP-GC	TYR-Au
E_{pa} [V] vs. NHE	0.600	0.505	0.592	0.616
E_{pc} [V] vs. NHE	0.269	0.300	0.232	0.250
ΔE_p [V]	0.331	0.295	0.360	0.366
I_{pa} [mA/cm^2]	0.046	0.048	0.029	0.016
I_{pc} [mA/cm^2]	−0.046	−0.049	−0.056	−0.026
$\lvert I_{pc}/I_{pa}\rvert$	1	1.021	1.931	1.625

The coverage of AuNP was about 13%.

reaction but also by the enzymatic reaction. Also those two peaks were linearly correlated with (scan rate)$^{1/2}$ implying a diffusion limited process (Fig. 6(b)). Another cathodic peak at −0.4 V vs. NHE was attributed to the reduction of dissolved oxygen, which was obtained from the voltammograms in the absence of phenol.

Table 1 shows comparison of redox signals of bare, AuNP-, and TYR-AuNP-GC and TYR-Au electrodes in the presence of catechol. The data were obtained from the CV measurements. When AuNPs were deposited at the electrode, the anodic and cathodic peak current (I_{pa} and I_{pc}) increased while peak separation, ΔE_p, decreased. After enzyme immobilization, I_{pa} decreased while I_{pc} and ΔE_p increased. The amount of catechol oxidized by electrochemical reaction decreased while the amount of quinone reduced by electrochemical reaction increased due to the amplification nature of substrate recycling process between TYR and electrode [31]. The shift of E_{pc} induced the increase of ΔE_p and it lowers the applied potential. From the higher current response and $|I_{pc}/I_{pa}|$ of TYR-AuNP-GC electrode than TYR-Au electrode, it was confirmed that

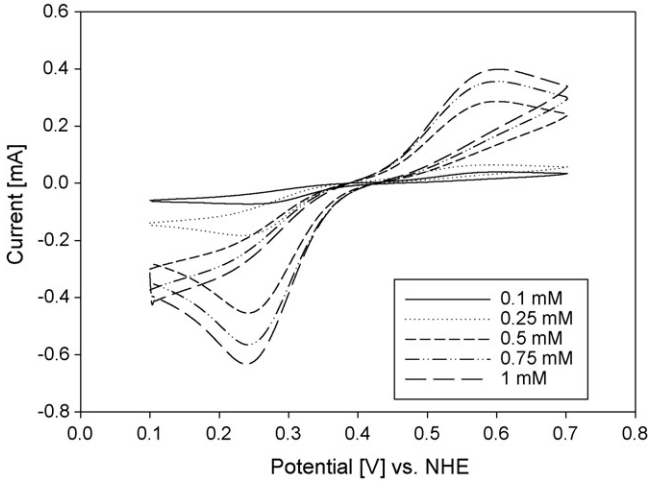

Fig. 7. The cyclic voltammograms of TYR-AuNP-GC electrode for various concentrations of catechol in O_2-saturated PBS (0.1 M, pH 7) at 25 mV/s.

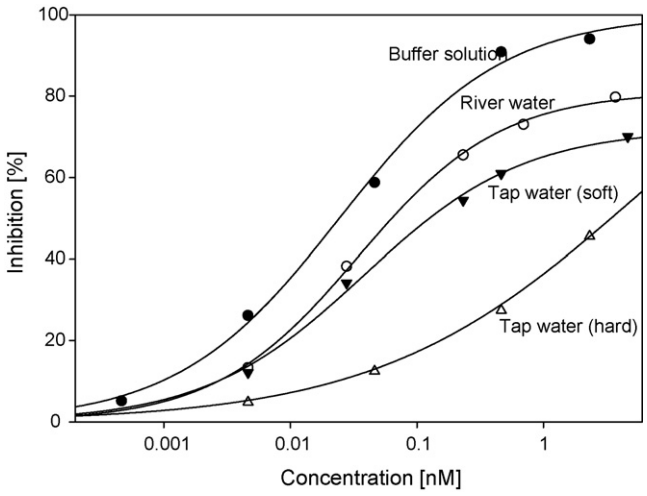

Fig. 8. Inhibition effect of TYR-AuNP-GC electrode with the addition of atrazine in buffer solution (pH 7, 13.9 mS/cm), filtered river water (pH 7.1, 0.17 mS/cm), soft tap water (pH 7.1, 0.10 mS/cm, total hardness 20 ppm as $CaCO_3$), and hard tap water (pH 6.9, 0.13 mS/cm, total hardness 128 ppm as $CaCO_3$) (flow rate: 1.2 mL/min, incubation time: 200 s, catechol: 1 mM).

AuNPs improved the current signal as well as high efficiency of the TYR immobilization [32]. In order to confirm the current response of the TYR immobilized electrode to addition of catechol, cyclic voltammograms were measured with the increasing concentration of catechol. As shown in Fig. 7, the redox peak current of TYR-AuNP-GC electrode increased with the increasing concentration of catechol, while the increasing rate diminished at higher concentrations.

3.5. Application of the TYR-AuNP-GC electrode in various water samples

To determine the concentration of pesticide in various water samples, a quantitative relationship between the inhibition percentage (I %) and the pesticide concentration (C) should be established. The relationship at the TYR-AuNP-GC electrode is identified by the amperometric response of the electrode to a substrate prior to and after the exposure to the pesticides, A_0 and A_i, respectively. Thus the inhibition percentage was calculated by the equation: $I(\%) = (1 - (A_i/A_0)) \times 100$. The inhibition experiments were conducted in a flow cell system under the optimized conditions, flow rate = 1.2 mL/min, substrate concentration = 1 mM, and incubation time = 200 s. The TYR-AuNP-GC electrode was tested using buffer solution, filtered river water from Youngsan River, soft and hard tap water samples. From the results, a logical relationship between I and C for atrazine in various water samples was obtained (Fig. 8). Based on the report on the reversible and competitive inhibition mechanism of TYR by atrazine, the inhibition curves were fitted and it was known that the inhibition of the immobilized TYR is controlled by the enzyme kinetics and the affinity of the immobilized TYR to each pesticides was estimated from b, related with K_I (equilibrium constant in the formation of enzyme–pesticide complex): tap water < soft tap water < river water < buffer solution (Table 2). A reasonable detection range was from 0.001 to 0.5 ng/mL showing 20–90% of inhibition in buffer solution. Although R.S.D. at a lower concentration was a little higher than that at a higher concentration, the intra-assay R.S.D. values in the range of 2.7–14.0% ($n = 5$). As shown in Fig. 8, the inhibition effects in river and soft tap water were slightly reduced due to lower conductivity and ionic strength compared to the buffer solution. Still, the electrode performed reasonably in river and soft tap water samples to measure the pesticide concentrations from the inhibition percentage. When the enzyme electrode measurement was performed directly in the natural water sample in the presence of total hardness of $CaCO_3$ of about 128 ppm, the lowest inhibition percentage value was obtained. This was probably due to the higher hardness concentration, which retards the rate of response [33]. Various types of TYR electrodes for atrazine detection have been reported; McArdle and Persaud described the TYR-Au electrode which has 1.08 μg/mL of LOD [34]; Védrine et al. reported TYR-PEDT-GC electrode for 5–40 μg/mL (LOD = 1 μg/mL); El Kaoutit et al. developed the TYR-PPy-GC electrode for 0.05–0.5 μg/mL of detection range and 0.1 μg/mL of LOD [35]; Campanella et al. presented TYR-Kappa-carrageenan gel electrode detecting 0.432 ng/mL–43.2 μg/mL (LOD = 0.1 ng/mL, R.S.D. = 8%) [36]. In this study, the detection limit and range was observed as 0.35 pg/mL and 0.001–0.5 ng/mL, respectively. In addition, it was observed that the prepared electrode is possible to use approximately 10 continuous assays without loss of enzyme activity.

Table 2
The fitted lines were determined according to the theoretical model, $I(\%) = a/((b/C_I) + 1) \times 100$, $b = K_I(1 + (C_s/K))$, where C_s and K were determined as 1 and 0.82 mM from the experiments in the flow cell, respectively

	Buffer solution	River water	Tap water (soft)	Tap water (Hard)
a	1.00	0.81	0.72	1.10
K_I	1.13×10^{-2}	1.44×10^{-2}	1.49×10^{-2}	6.11×10^{-1}

4. Conclusion

In this study, AuNPs were electrodeposited by controlling potential and time to improve the current response of the tyrosinase based enzyme electrode. The coverage of AuNPs was optimized with respect to the sensor signal of TYR-AuNP-GC electrode. A sensitive current response was obtained at the TYR-AuNP-GC electrode attributed by the use of AuNPs and the feasibility of the electrode for pesticide measurements was successively demonstrated.

Acknowledgment

This work was supported by the Research Center for Biomolecular Nanotechnology at GIST.

References

[1] W.K. Lafi, Z. Al-Qodah, Combined advanced oxidation and biological treatment processes for the removal of pesticides from aqueous solutions, J. Hazard. Mater. 137 (2006) 489–497.

[2] H.J. Yeh, C.Y. Chen, Toxicity assessment of pesticides to Pseudokirchneriella subcapitata under air-tight test environment, J. Hazard. Mater. 131 (2006) 6–12.
[3] R. Zhou, L. Zhu, K. Yang, Y. Chen, Distribution of organochlorine pesticides in surface water and sediments from Qiantang River, East China, J. Hazard. Mater. 137 (2006) 68–75.
[4] G.R.P. Malpass, D.W. Miwa, S.A.S. Machado, P. Olivi, A.J. Motheo, Oxidation of the pesticide atrazine at DSA® electrodes, J. Hazard. Mater. 137 (2006) 565–572.
[5] C. Badellino, C.A. Rodrigues, R. Bertazzoli, Oxidation of pesticides by in situ electrogenerated hydrogen peroxide: study for the degradation of 2,4-dichlorophenoxyacetic acid, J. Hazard. Mater. 137 (2006) 856–864.
[6] H. Mercan, E. Yilmaz, R. Inam, Determination of insecticide pymetrozine by differential pulse polarography/application to lake water and orange juice, J. Hazard. Mater. 141 (2007) 700–706.
[7] N. Daneshvar, S. Aber, A. Khani, A.R. Khataee, Study of imidaclopride removal from aqueous solution by adsorption onto granular activated carbon using an on-line spectrophotometric analysis system, J. Hazard. Mater. 144 (2007) 47–51.
[8] H. Cheng, W. Xu, J. Liu, H. Wang, Y. He, G. Chen, Pretreatment of wastewater from triazine manufacturing by coagulation, electrolysis, and internal microelectrolysis, J. Hazard. Mater. 146 (2007) 385–392.
[9] B. Prieto-Simón, M. Campàs, S. Andreescu, J.-L. Marty, Trends in flow-based biosensing systems for pesticide assessment, Sensors 6 (2006) 1161–1186.
[10] K.R. Rogers, Recent advances in biosensor techniques for environmental monitoring, Anal. Chim. Acta 568 (2006) 222–231.
[11] L.Y. Gorelik, M.V. Voinova, Mechanically mediated electron transfer in model metallo-enzyme interfaces, Biosens. Bioelectron. 22 (2006) 405–408.
[12] A. Salimi, E. Sharifi, A. Noorbakhsh, S. Soltanian, Immobilization of glucose oxidase on electrodeposited nickel oxide nanoparticles: direct electron transfer and electrocatalytic activity, Biosens. Bioelectron. 22 (2007) 3146–3153.
[13] D. Tang, R. Yuan, Y. Chai, Biochemical and immunochemical characterization of the antigen – antibody reaction on a non-toxic biomimetic interface immobilized red blood cells of crucian carp and gold nanoparticles, Biosens. Bioelectron. 22 (2007) 1116–1120.
[14] I. Willner, R. Baron, B. Willner, Integrated nanoparticle–biomolecule systems for biosensing and bioelectronics, Biosens. Bioelectron. 22 (2007) 1841–1852.
[15] V. Carralero Sanz, M. Luz Mena, A. Gonzalez-Cortes, P. Yanez-Sedeno, J.M. Pingarron, Development of a tyrosinase biosensor based on gold nanoparticles-modified glassy carbon electrodes, application to the measurement of a bioelectrochemicla polyphenols index in wines, Anal. Chim. Acta 528 (2005) 1–8.
[16] C. Vedrine, S. Fabiano, C. Tran-Minh, Amperometric tyrosinase based biosensor using an electrogenerated polythiophene film as an entrapment support, Talanta 59 (2003) 535–544.
[17] J. Yu, S. Liu, H. Ju, Mediator-free phenol sensor based on titania sol–gel encapsulation matrix for immobilization of tyrosinase by a vapor deposition method, Biosens. Bioelectron. 19 (2003) 509–514.
[18] B. Wang, J. Zhang, S. Dong, Silica sol–gel composite film as an encapsulation matrix for the construction of an amperometric tyrosinase-based biosensor, Biosens. Bioelectron. 15 (2000) 397–402.
[19] S. Campuzano, B. Serra, M. Pedero, F.J. Manuel de Villena, J.M. Pingarron, Amperometric flow-injection determination of phenolic compounds at self-assembled monolayer-based tyrosinase biosensors, Anal. Chim. Acta 494 (2003) 187–197.
[20] K. Streffer, E. Vijgenboom, A.W.J.W. Tepper, A. Makower, E.W. Scheller, G.W. Canter, U. Wollenberger, Determination of phenolic compounds using recombinant tyrosinase from Streptomyces antibioticus, Anal. Chim. Acta 427 (2001) 201–210.
[21] J. Zhang, M. Kambayashi, M. Oyama, A novel electrode surface fabricated by directly attaching gold nanospheres and nanorods onto indium tin oxide substrate with a seed mediated growth process, Electrochem. Commun. 6 (2004) 683–688.
[22] E. Katz, I. Willner, J. Wang, Electroanalytical and bioanalytical systems based on metal and semiconductor nanoparticles, Electroanalysis 16 (2004) 19–44.
[23] G. Sandmann, H. Dietz, W.J. Plieth, Preparation of silver nanoparticles on ITO surfaces by a double-pulse method, Electroanal. Chem. 491 (2000) 78–86.
[24] M. Ueda, H. Dietz, A. Anders, H. Kneppe, A. Meixner, W. Plieth, Double-pulse technique as an electrochemical tool for controlling the preparation of metallic nanoparticles, Electrochim. Acta 48 (2002) 377–386.
[25] G. Trejo, A.F. Fil, I. Gonzalez, Temperature effect on the electrocrystallization process of gold in ammoniacal medium, J. Electrochem. Soc. 142 (1995) 3404–3408.
[26] S. Liu, D. Leech, H. Ju, Application of colloidal gold in protein immobilization, electron transfer, and biosensing, Anal. Lett. 36 (2003) 1–19.
[27] M.O. Finot, G.D. Braybrook, M.T. McDermott, Characterization of electrochemically deposited gold nanocrystals on glassy carbon electrode, J. Electroanal. Chem. 466 (1999) 234–241.
[28] U. Schmidt, M. Donten, J.G. Osteryoung, Gold electrocrystallization on carbon and highly oriented pyrolytic graphite from concentrated solutions of LiCl, J. Electrochem. Soc. 144 (1997) 2013–2021.
[29] E. Budevski, G. Staikov, W.J. Lorenz, Electrocrystallization: nucleation and growth phenomena, Electrochim. Acta 45 (2000) 2559–2574.
[30] J. Li, J. Yan, Q. Deng, G. Cheng, S. Dong, Viologen-thiol semf-assembled monolayers for immobilized horseradish peroxidase at gold electrode surface, Electrochim. Acta 42 (1997) 961–967.
[31] O. Shulge, J.R. Kirchhoff, An acetylcholinesterase enzyme electrode stabilized by an electrodeposited gold nanoparticle layer, Electrochem. Commun. 9 (2007) 935–940.
[32] T.H. Huang, T. Kuwana, A. Warsinke, Analysis of thiols with tyrosinase-modified carbon paste electrodes based on blocking of substrate recycling, Biosens. Bioelectron. 17 (2002) 1107–1113.
[33] V.G. Andreou, Y.D. Clonis, Novel fiber-optic biosensor based on immobilized glutathione S-transferase and sol–gel entrapped bromcresol green for the determination of atrazine, Anal. Chim. Acta 460 (2002) 151–161.
[34] F.A. McArdle, K.C. Persaud, Development of an enzyme-based biosensor for atrazine detection, Analyst 118 (1993) 419–423.
[35] M. El Kaoutit, D. Bouchta, H. Zejli, N. Izaoumen, K.R. Temsamani, A simple conducting polymer-based biosensor for the detection of atrazine, Anal. Lett. 37 (2004) 1671–1681.
[36] L. Campanella, A. Bonanni, E. Martini, N. Todini, M. Tomassetti, Determination of triazine pesticides using a new enzyme inhibition tyrosinase OPEE operating in chloroform, Sens. Actuators B 112 (2005) 505–514.